

# Phase transitions of the Dicke model: a unified perspective

Pragna Das<sup>1</sup> and Auditya Sharma<sup>1</sup>

<sup>1</sup>*Indian Institute of Science Education and Research Bhopal 462066 India*

The Dicke model exhibits a variety of phase transitions. The quantum phase transition from the normal phase to the super-radiant phase is marked by a dramatic change in the scaling of the participation ratio. We find that the ground state in the super-radiant phase exhibits multifractality manifest in the participation ratio scaling as the square root of the full Hilbert space dimension. The thermal phase transition temperature, for which we obtain an exact analytical expression, is strikingly captured by the mutual information between two spins. In the excited state quantum phase transition within the super-radiant phase, we discover a new upper cut-off energy; the central energy band between the lower and upper cut-off energies shows distinctly different behaviour. This finding is corroborated with the aid of several *eigenvector* properties: von Neumann entanglement entropy between spins and bosons, the mean photon number, concurrence between two spins, and participation ratio. Thus we obtain a unified picture for the three different kinds of phase transitions.

The Dicke model, which incorporates the interactions of an ensemble of  $N$  two-level atoms via dipole coupling with a single bosonic mode [1–3] has its origin in quantum optics, but has found application in a wide range of fields from quantum chaos to quantum entanglement [4–17] to scrambling and thermalization [18]. Besides possessing an intimate connection to experiments [19–21], the Dicke model is a testbed for a variety of phase transitions [22]. Although a lot is known about these different transitions, the literature presents a rather scattered treatment of them [22–29]. In this Letter, we provide a transparent unified picture of three different kinds of phase transitions in the Dicke model.

The nature of the ground state of the Dicke model is dramatically different depending on the magnitude of the coupling between the atoms and the field. While for small coupling, in the normal phase, the average photon number in the ground state is close to zero, when the coupling is greater than a critical value, in the super-radiant phase, the ground state mean photon number scales linearly with the number of atoms [22–25]. Entanglement properties [15–17] offer clear signatures of this quantum phase transition [30–35] (QPT). Furthermore, a study of level statistics shows that the system in fact also undergoes a transition from quasi-integrable to quantum chaotic [16] at the QPT. In this Letter, with the aid of a careful study of the participation ratio [36] of the ground state, we show how the normal to super-radiant phase transition is really a localization-to-multifractal transition. We find that in the super-radiant phase, the ground state participation ratio scales as the square root of the full Hilbert space dimension.

The Dicke model also exhibits a thermal phase transition (TPT) which was realized many decades ago [26, 27]. When the coupling is greater than the critical coupling, as the temperature is increased, we see a transition back from the super-radiant to the normal phase [28]. In this Letter, we obtain an exact analytical expression for the transition temperature. Generalizing the approach of Wang and Hioe [27], we write down the partition function

as a double integral. The transition temperature is identified to be the point at which the method of steepest descent used to evaluate the integral in the thermodynamic limit breaks down. Furthermore, just like entanglement in the ground state marks the quantum phase transition, we show how the mutual information (MI) between atoms offers a striking signature at the thermal phase transition.

The Dicke model also exhibits an excited state quantum phase transition (ESQPT), a term that is used to denote criticality in the excited states of a quantum system [28, 29, 37–40]. The ESQPT, which is a generalization of the QPT, and is characterized by abrupt variations of the energy and other excited state properties at a sharp critical value of the energy [41] must be viewed in the backdrop of the tremendous recent interest in the properties of excited states [37, 42–48] of quantum systems. In the present Letter, we uncover how the ESQPT of the Dicke model affects not only energy levels below a certain lower cut-off, but also the top-lying energy levels above a second *upper* cut-off, a feature that has apparently been hitherto unnoticed in the literature [18, 46]. Strikingly, in contrast to prior studies, we are able to identify these features with the aid of several *eigenstate* properties: von Neumann entanglement entropy (VNEE), the mean photon number, concurrence and *PR*. Supporting evidence comes from eigenvalue properties like level statistics [49] and the consecutive level spacing ratio [50] considering both the whole and different parts of the spectrum.

The Hamiltonian of the Dicke model is

$$\mathcal{H} = \omega a^\dagger a + \omega_0 J_z + \frac{g}{\sqrt{2j}}(a + a^\dagger)(J_+ + J_-) \quad (1)$$

where  $a$  and  $a^\dagger$  are bosonic operators satisfying the commutation relation:  $[a, a^\dagger] = 1$  in units where  $\hbar = 1$ .  $\omega$  is the single-mode frequency of the bosonic field while  $\omega_0$  is the level splitting of the atoms, and  $g$  is the coupling strength of the light-matter interaction. The angular momentum operators  $J_{\pm, z} = \sum_{i=1}^{2j} \frac{1}{2} \sigma_{\pm, z}^{(i)}$  cor-

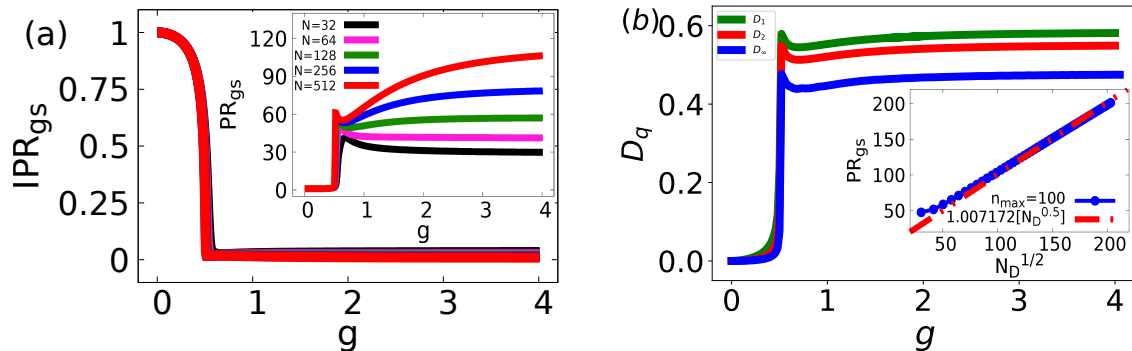


Figure 1. (a) The inverse participation ratio ( $IPR$ ) of the ground state as a function of coupling  $g$ . The inset shows a similar plot for participation ratio ( $PR$ ). (b) Multifractal dimension  $D_q$  ( $q = 1, 2, \infty$ ) of the ground state as a function of  $g$ . The inset shows the scaling of  $PR$  with atom number  $N$  for the ground state at  $g = 4.0$ . In all the figures, we set  $N = 512$ ,  $n_{\max} = 32$ .

respond to a pseudospin with length  $j$ , composed of  $N = 2j$  spin- $\frac{1}{2}$  atoms described by Pauli matrices  $\sigma_{\pm,z}^{(i)}$  acting on site  $i$  and satisfy the commutation relations:  $[J_z, J_\pm] = \pm J_\pm$ ,  $[J_+, J_-] = 2J_z$ . The basis of the full Hilbert space of the system is  $\{|n\rangle \otimes |j, m\rangle\}$  where  $|n\rangle$  are the bosonic basis states satisfying  $a^\dagger a |n\rangle = n |n\rangle$  and  $|j, m\rangle$  are the Dicke states satisfying  $J_\pm |j, m\rangle = \sqrt{j(j+1) - m(m \pm 1)} |j, m \pm 1\rangle$ ,  $J_z |j, m\rangle = m |j, m\rangle$ . In our work, we take  $N$  to be even, and consider the symmetric subspace which fixes  $j = \frac{N}{2}$ , and thus  $m$  takes the  $(N+1)$  values  $(-\frac{N}{2}, \dots, 0, \dots, \frac{N}{2})$ . We also truncate the bosonic mode to take the values  $n = 0, 1, \dots, n_{\max}$ . Thus the dimension of the Hilbert space is given by  $N_D = (N+1)(n_{\max}+1)$ . In the thermodynamic limit the system shows a second-order quantum phase transition from the normal phase (NP) to the super-radiant phase (SP) at  $g = \frac{\sqrt{\omega\omega_0}}{2}$  ( $= g_c$ ) [16]. In all our numerical calculations we have set  $\omega = \omega_0 = 1$  and hence  $g_c = 0.5$ .

*Quantum phase transition:* The inverse participation ratio ( $IPR$ ) of an eigenstate  $|\psi\rangle = \sum_j^{N_D} \psi_j |j\rangle$  (where  $N_D$  is the Hilbert space dimension) defined as:

$$IPR = \sum_{j=1}^{N_D} |\psi_j|^4. \quad (2)$$

It is useful to quantify the degree of delocalization of the eigenstate. Fig. 1(a) shows an exact diagonalization study of the  $IPR$  of the ground state as  $g$  is varied; we observe that it is close to one in the NP and close to zero in the SP. Thus we see that the ground state is localized in the NP whereas it is extended in nature in the SP. Echoes of these features are also found in both static and dynamical studies of a variety of other measures of quantum correlations (see supplementary section). The inset of Fig. 1(a) studies the participation ratio  $PR$  (which is the inverse of  $IPR$ ), as a function of the coupling  $g$  and it shows a phase transition from NP where it takes values close to zero, to SP with a sharp transition to a non-zero value at the critical coupling. We plot the  $PR$  for differ-

ent atom number  $N$  and notice that in the SP the value of  $PR$  increases with  $N$ .

A finer understanding of the localization properties may be obtained by studying the multifractal dimension [51, 52]:

$$D_q = \frac{S_q}{\ln(N_D)} \quad (3)$$

where  $S_q = \frac{1}{1-q} \ln \left( \sum_{j=1}^{N_D} |\psi_j|^{2q} \right)$  is known as the  $q$ -dependent participation entropy. In the Shannon limit ( $q = 1$ ),  $S_1 = \sum_j |\psi_j|^2 \ln(|\psi_j|^2)$ , while  $q = 2$  yields the usual  $IPR$  with  $S_2 = -\ln(IPR)$ .  $S_\infty$  is determined by the maximum value of the densities  $p_{\max} = \max_j |\psi_j|^2$  and  $D_\infty = -\frac{\ln(p_{\max})}{\ln(N_D)}$ . For a perfectly delocalized state  $S_q = \ln(N_D)$  (when  $N_D$  is large) and hence  $D_q = 1$  for all  $q$ . On the other hand for a localized state  $S_q = \text{constant}$  and  $D_q = 0$ . In an intermediate situation, wave functions are extended but non-ergodic with  $S_q = D_q \ln(N_D)$  where  $0 < D_q < 1$  and the state is multifractal. In Fig. 1(b) we show  $D_1$ ,  $D_2$  and  $D_\infty$  for the ground state as a function of the coupling parameter  $g$ . In the NP  $D_q \approx 0$  hence we can say that the ground state is localized in the NP. Contrastingly in the SP,  $0 < D_q < 1$  with  $D_1 > D_2 > D_\infty$  ( $D_1 \approx 0.58$ ,  $D_2 \approx 0.55$ ,  $D_\infty \approx 0.47$ ), with a sharp transition at the critical point. In the inset of Fig. 1(b) we show that at  $g = 4.0$ ,  $PR$  goes as the square root of the Hilbert space dimension. Hence we find that the SP is neither perfectly delocalized nor localized, and in fact displays multifractal character [51]. Given the intense current interest in multifractal states [53–55], this discovery in a familiar model is an exciting finding.

*Thermal phase transition:* To compute the partition function ( $Z = \text{Tr}(e^{-\frac{\mathcal{H}}{k_B T}})$ ) of the Dicke Hamiltonian it is useful to first write it in units of  $\omega$  as:

$$\tilde{\mathcal{H}} = \frac{\mathcal{H}}{\omega} = a^\dagger a + \sum_{j=1}^N \frac{\epsilon}{2} \sigma_j^z + \frac{\lambda}{\sqrt{N}} \sum_{j=1}^N (a + a^\dagger) \sigma^x \quad (4)$$

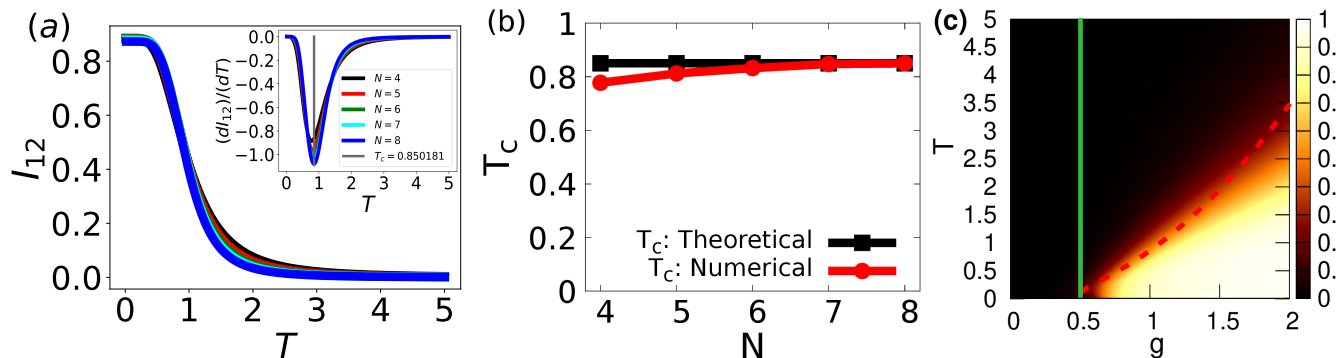


Figure 2. (a) Mutual information (MI) of two spins as a function of temperature at  $g = 1.0$ , with the inset showing the numerical derivative of MI wrt temperature  $\frac{dI_{12}}{dT}$ . (b) The red line denotes the critical temperature as a function of atom number  $N$ , while the black line is the theoretical value ( $T_c = 0.850181$ ) for  $g = 1.0$ . (c) Mutual information of two spins as a function of coupling  $g$  and temperature  $T$ . The parameters are  $N = 6$ ,  $n_{max} = 10$ . The black region corresponds to the NP, and the white region to the SP. The solid line corresponds to  $g_c$  and the dashed line denotes the critical temperature theoretically calculated in Eqn. 6. In all the plots  $\omega = \omega_0 = 1$ .

where  $\epsilon = \frac{\omega_0}{\omega}$  and  $\lambda = \frac{g}{\omega}$ . Following the method of Wang and Hioe [27] (who studied the Dicke model within the rotating wave approximation), the computation of the partition function reduces to the evaluation of a double integral (see supplementary section):

$$Z(N, T) = \int \frac{d^2\alpha}{\pi} e^{-\beta|\alpha|^2} \left( 2 \cosh \left[ \frac{\beta\epsilon}{2} \left[ 1 + \frac{16\lambda^2\alpha^2}{\epsilon^2 N} \right]^{1/2} \right] \right)^N \quad (5)$$

which in the thermodynamic limit ( $N \rightarrow \infty$ ), may be carried out with the aid of the method of steepest descent, within the super-radiant phase. Tracking the point at which the method breaks down (see supplementary section), we obtain an exact expression for the transition temperature:

$$T_c = \frac{1}{\beta_c} = \left( \frac{\omega_0}{2\omega} \right) \frac{1}{\tanh^{-1} \left( \frac{\omega\omega_0}{4g^2} \right)}. \quad (6)$$

The critical temperature expression is meaningful only when  $g > g_c$ . When  $g < g_c$ , the system is in the normal phase at all temperatures. When  $g > g_c$ , it is only above the critical temperature that the system is in the normal phase, while for  $T < T_c$  the system is in the super-radiant phase.

The mutual information (MI) between two atoms  $I_{12}$  proves to be a very useful quantity to study. Using the single-spin reduced density matrices  $\rho_1, \rho_2$  and the two-spin reduced density matrix  $\rho_{12}$ , we can work out the von Neumann entropies  $S_{1,2} = -Tr(\rho_{1,2} \ln(\rho_{1,2}))$ ,  $S_{12} = -Tr(\rho_{12} \ln(\rho_{12}))$  from which the mutual information [56–59] is immediately written down:

$$I_{12} = S_1 + S_2 - S_{12}. \quad (7)$$

In Fig. 2(a) we show  $I_{12}$  as a function of temperature at  $g = 1$  ( $g > g_c$ ). At low temperatures in the SP,  $I_{12}$  takes a

value close to unity while at high temperatures in the NP,  $I_{12}$  drops to a value close to zero, with a dramatic drop happening at a temperature close to the transition temperature. For a finer understanding of the variation of the mutual information across the transition, we study in the inset of Fig. 2(a) the first-order temperature derivative  $\frac{dI_{12}}{dT}$ , for different atom numbers. We observe that the temperature at which the derivative takes the minimum value is consistent with the transition temperature  $T_c$ , denoted by the vertical line. Fig. 2(b) confirms that as the number of atoms is increased the temperature at the minimum does indeed approach the theoretically obtained critical temperature. From the surface plot of the MI as a function of  $g$  and  $T$  in Fig. 2(c), it is clear that for  $g < g_c$  there is no phase transition, but for  $g > g_c$  there exists a critical temperature  $T_c$  at which the system changes from the super-radiant phase ( $T < T_c$ ) to the normal phase ( $T > T_c$ ). While it is widely known that entanglement in the ground state signals the QPT, our work shows that despite also including classical correlations, the mutual information between atoms offers a striking signature at the thermal phase transition.

*ESQPT:* The Dicke model exhibits an excited state quantum phase transition in the super-radiant phase. When  $g > g_c$ , it has been reported [18, 46] that the eigenvalues above a cut-off energy  $E_c$  behave in a distinctly different manner in comparison with the eigenvalues below the cut-off. We find that in fact there is not just a lower cut-off, but also an upper cut-off. Our data show that we must study separately the eigenvalues drawn from a central band that comprises of energy levels between a lower and upper cut-off. The lower and upper energy bands show different behaviour. While eigenvalue properties like level-statistics and gap ratio provide supporting evidence (see supplementary section), we highlight how *eigenstate properties* offer a striking demonstration of this picture.

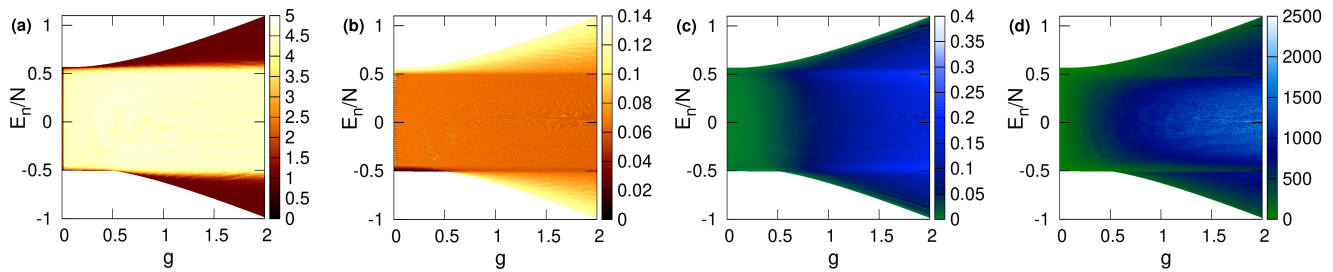


Figure 3. (a) Von Neumann entanglement entropy between the atoms and the bosons as a function of coupling strength  $g$  and the energy density  $E_n/N$  (eigenenergy divided by the atom number  $N$ ) of the DM. (b) Similar plot for mean photon number, (c) for concurrence between any two atoms and (d) participation ratio of the eigenstates. The parameters for all the four plots are  $N = 512$ ,  $n_{\max} = 32$ .

In Fig. 3(a) we show the VNEE [15] between spins and bosons:

$$S = -\text{Tr}\left(\rho_{\text{boson}} \log_2 \rho_{\text{boson}}\right), \quad (8)$$

for all the eigenstates of the Dicke model. Here  $\rho_{\text{boson}} = \text{Tr}_{\text{atom}}\rho$  is the reduced density matrix of the bosonic part. We observe two cut-off energies: (i) lower cut-off energy (corresponding to the ground state energy at  $g = g_c$ ) and (ii) upper cut-off energy (corresponding to the maximum energy for  $g = 0$ ). The value of VNEE is larger in the eigenstates of the central band in comparison with that of the top and bottom bands. Thus the eigenstates carry a clear signature of the two excited state quantum phase transitions when  $g > g_c$ . In Fig. 3(b) we show a similar plot for the mean photon number [16],  $\langle a^\dagger a \rangle$  which is scaled by the pseudospin length  $j$  of the system. It carries information pertaining to the bosonic part of the eigenstates. In the middle band the value of the mean photon number is comparatively lower than that of the other two bands. However, we observe that neither the VNEE between the atoms and the bosons, nor the mean photon number is able to distinguish between the  $g < g_c$  and  $g > g_c$  regions of the middle band. A study of the entanglement between atoms provides useful further perspective.

The concurrence [60–63] between (any) two atoms is given by:

$$C = \max\{0, \lambda_1 - \lambda_2 - \lambda_3 - \lambda_4\}, \quad (9)$$

where  $\lambda_i$  are the square roots of the eigenvalues of the matrix product,  $\tilde{\rho}_{12} = \rho_{12}(\sigma_{1y} \otimes \sigma_{2y})\rho_{12}^*(\sigma_{1y} \otimes \sigma_{2y})$ , in descending order ( $\lambda_1 > \lambda_2 > \lambda_3 > \lambda_4$ ). Here  $\rho_{12}^*$  denotes complex conjugation of  $\rho_{12}$ , and  $\sigma_{iy}$  are Pauli matrices for two-level systems. In Fig. 3(c) we plot concurrence between two atoms for the whole spectrum as a function of  $g$ . We observe that in addition to showing a signature of the ESQPT in the super-radiant phase, concurrence is also able to distinguish the eigenstates of the middle band in the  $g < g_c$  region and the  $g > g_c$  region. In the NP, the concurrence value of the central states is comparatively

smaller than that for the central states of the SP. Again the value of concurrence in the bottom and top bands of the super-radiant phase is a bit lower than that of the central band. Fig. 3(d) shows the participation ratio of all the eigenstates as a function of coupling parameter  $g$ . We are able to identify the ESQPT, which divides the whole spectrum into three bands: top, bottom, and central. In the NP ( $g < g_c$ ), the whole region shows a uniform comparatively small value of  $PR$ . On the other hand in the SP ( $g > g_c$ ) while the central band exhibits a larger value of  $PR$ , the top and bottom bands show mixed behaviour, although they resemble the NP more than the SP.

*Summary:* We study the phase transitions (QPT, TPT, ESQPT) of the Dicke model, with the aid of a number of measures of localization, entanglement and mutual information. Different quantities are more suitable for the different kinds of phase transitions involved, and a comprehensive look at all of them helps us obtain a unique overall big-picture of the Dicke model. We are thus able to provide a unified perspective of three different kinds of phase transitions. The  $IPR$  for the ground state shows a sharp phase transition at  $g_c$ ; while in the NP the ground state behaves like a localized state, the ground state in the SP is not localized. A careful study of the scaling of  $PR$  (for the ground state in the SP) with the dimension  $N_D$  of the full Hilbert space reveals that the  $PR$  scales as  $\sqrt{N_D}$  suggesting multifractal character. In the  $g > g_c$  region there exists some critical temperature  $T_c$ , above which the SP disappears and the system goes into the NP whereas for  $g < g_c$  the system remains in the NP for all temperatures. We obtain a closed-form expression for the transition temperature in the super-radiant phase, and numerically verify that the mutual information between two atoms provides a useful signature at the transition. Thus at the temperature transition, the mutual information proves to be a worthy generalization of entanglement, which marks the ground state QPT. We find that in the super-radiant phase, the ESQPT is signalled not just by a lower energy cut-off, but an upper energy cut-off as well. The

ESQPT is studied with the aid of VNEE, mean photon number, concurrence and  $PR$ . For the VNEE and mean photon number the whole central band is uniform, with no distinction between  $g < g_c$  and  $g > g_c$  regions. We find that concurrence and  $PR$  reveal more structure. In addition to showing a signature of the ESQPT in the SP, these quantities are also able to distinguish the eigenstates of the central band between the  $g < g_c$  region and  $g > g_c$  region. Hence we are able to present various phase transitions in the DM in terms of several quantities that measure localization, multifractality, mutual information and entanglement. It would be interesting to extend the ideas in this study to other spin-boson models, to open quantum systems that include a bosonic bath, and models with a periodic drive.

### ACKNOWLEDGMENTS

We are thankful to Devendra Singh Bhakuni, Nilanjan Roy, Suhas Gangadharaiah and Sebastian Wüster for fruitful comments and discussions. P.D. is grateful to IISERB for the PhD fellowship. A.S acknowledges financial support from SERB via the grant (File Number: CRG/2019/003447), and from DST via the DST-INSPIRE Faculty Award [DST/INSPIRE/04/2014/002461].

- 
- [1] S. Haroche, in *Conference on Coherence and Quantum Optics* (Optical Society of America, 2007) p. CTuF2.
- [2] H. Kimble, Q. Turchette, N. P. Georgiades, C. Hood, W. Lange, H. Mabuchi, E. Polzik, and D. Vernooy, in *Coherence and Quantum Optics VII* (Springer, 1996) pp. 203–210.
- [3] M. Mirhosseini, E. Kim, X. Zhang, A. Sipahigil, P. B. Dieterle, A. J. Keller, A. Asenjo-Garcia, D. E. Chang, and O. Painter, *Nature* **569**, 692 (2019).
- [4] K. Furuya, M. C. Nemes, and G. Q. Pellegrino, *Phys. Rev. Lett.* **80**, 5524 (1998).
- [5] A. Lakshminarayan, *Phys. Rev. E* **64**, 036207 (2001).
- [6] J. N. Bandyopadhyay and A. Lakshminarayan, *Phys. Rev. Lett.* **89**, 060402 (2002).
- [7] J. N. Bandyopadhyay and A. Lakshminarayan, *Phys. Rev. E* **69**, 016201 (2004).
- [8] A. Tanaka, H. Fujisaki, and T. Miyadera, *Phys. Rev. E* **66**, 045201 (2002).
- [9] M. Žnidarič and T. c. v. Prosen, *Phys. Rev. A* **71**, 032103 (2005).
- [10] P. Jacquod, *Phys. Rev. Lett.* **92**, 150403 (2004).
- [11] S. Ghose and B. C. Sanders, *Phys. Rev. A* **70**, 062315 (2004).
- [12] R. Demkowicz-Dobrzański and M. Kuś, *Phys. Rev. E* **70**, 066216 (2004).
- [13] Y. S. Weinstein and C. S. Hellberg, *Phys. Rev. Lett.* **95**, 030501 (2005).
- [14] A. Lakshminarayan and V. Subrahmanyam, *Phys. Rev. A* **67**, 052304 (2003).
- [15] N. Lambert, C. Emary, and T. Brandes, *Phys. Rev. Lett.* **92**, 073602 (2004).
- [16] C. Emary and T. Brandes, *Phys. Rev. E* **67**, 066203 (2003).
- [17] C. Emary and T. Brandes, *Phys. Rev. Lett.* **90**, 044101 (2003).
- [18] R. Lewis-Swan, A. Safavi-Naini, J. J. Bollinger, and A. M. Rey, *Nature communications* **10**, 1 (2019).
- [19] K. Baumann, R. Mottl, F. Brennecke, and T. Esslinger, *Phys. Rev. Lett.* **107**, 140402 (2011).
- [20] J. Klinder, H. Keßler, M. Wolke, L. Mathey, and A. Hemmerich, *Proceedings of the National Academy of Sciences* **112**, 3290 (2015).
- [21] M. P. Baden, K. J. Arnold, A. L. Grimsmo, S. Parkins, and M. D. Barrett, *Phys. Rev. Lett.* **118**, 199901 (2017).
- [22] P. Kirton, M. M. Roses, J. Keeling, and E. G. Dalla Torre, *Advanced Quantum Technologies* **2**, 1800043 (2019).
- [23] R. H. Dicke, *Physical review* **93**, 99 (1954).
- [24] E. Kadantseva, W. Chmielowski, and A. Shumovsky, in *Nonlinear Optics in Solids* (Springer, 1990) pp. 37–41.
- [25] P. Kirton and J. Keeling, *New Journal of Physics* **20**, 015009 (2018).
- [26] K. Hepp and E. H. Lieb, *Annals of Physics* **76**, 360 (1973).
- [27] Y. K. Wang and F. T. Hioe, *Phys. Rev. A* **7**, 831 (1973).
- [28] P. Pérez-Fernández and A. Relaño, *Phys. Rev. E* **96**, 012121 (2017).
- [29] G.-L. Zhu, X.-Y. Lü, S.-W. Bin, C. You, and Y. Wu, *Frontiers of Physics* **14**, 1 (2019).
- [30] S. S., draft ed. (CUP, 1998).
- [31] S. L. Sondhi, S. Girvin, J. Carini, and D. Shahar, *Reviews of modern physics* **69**, 315 (1997).
- [32] P. Cejnar, J. Jolie, and R. F. Casten, *Reviews of Modern Physics* **82**, 2155 (2010).
- [33] R. Casten and E. McCutchan, *Journal of Physics G: Nuclear and Particle Physics* **34**, R285 (2007).
- [34] J. Ma and X. Wang, *Phys. Rev. A* **80**, 012318 (2009).
- [35] A. Osterloh, L. Amico, G. Falci, and R. Fazio, *Nature* **416**, 608 (2002).
- [36] E. Tsukerman, *Phys. Rev. B* **95**, 115121 (2017).
- [37] M. Caprio, P. Cejnar, and F. Iachello, *Annals of Physics* **323**, 1106 (2008).
- [38] P. Stránský, M. Macek, and P. Cejnar, *Annals of Physics* **345**, 73 (2014).
- [39] P. Cejnar and P. Stránský, *Phys. Rev. E* **78**, 031130 (2008).
- [40] J. E. García-Ramos, P. Pérez-Fernández, and J. M. Arias, *Phys. Rev. C* **95**, 054326 (2017).
- [41] P. Cejnar, P. Stránský, M. Macek, and M. Kloc, *Journal of Physics A: Mathematical and Theoretical* **54**, 133001 (2021).
- [42] A. Pal and D. A. Huse, *Phys. Rev. B* **82**, 174411 (2010).
- [43] R. Nandkishore and D. A. Huse, *Annu. Rev. Condens. Matter Phys.* **6**, 15 (2015).
- [44] F. Alet and N. Laflorencie, *Comptes Rendus Physique* **19**, 498 (2018).
- [45] J. Karthik, A. Sharma, and A. Lakshminarayan, *Phys. Rev. A* **75**, 022304 (2007).
- [46] P. Pérez-Fernández, A. Relaño, J. M. Arias, P. Cejnar, J. Dukelsky, and J. E. García-Ramos, *Phys. Rev. E* **83**, 046208 (2011).
- [47] P. Pérez-Fernández, P. Cejnar, J. M. Arias, J. Dukelsky, J. E. García-Ramos, and A. Relaño, *Phys. Rev. A* **83**,

- 033802 (2011).
- [48] W. Beugeling, A. Andreanov, and M. Haque, *Journal of Statistical Mechanics: Theory and Experiment* **2015**, P02002 (2015).
- [49] D. Poilblanc, T. Ziman, J. Bellissard, F. Mila, and G. Montambaux, *EPL (Europhysics Letters)* **22**, 537 (1993).
- [50] Y. Y. Atas, E. Bogomolny, O. Giraud, and G. Roux, *Phys. Rev. Lett.* **110**, 084101 (2013).
- [51] N. Macé, F. Alet, and N. Laflorencie, *Phys. Rev. Lett.* **123**, 180601 (2019).
- [52] J. Lindinger, A. Buchleitner, and A. Rodríguez, *Phys. Rev. Lett.* **122**, 106603 (2019).
- [53] J. Lindinger and A. Rodríguez, *Phys. Rev. B* **96**, 134202 (2017).
- [54] M. Pino, V. E. Kravtsov, B. L. Altshuler, and L. B. Ioffe, *Phys. Rev. B* **96**, 214205 (2017).
- [55] M. Serbyn, Z. Papić, and D. A. Abanin, *Phys. Rev. B* **96**, 104201 (2017).
- [56] V. Vedral, *Phys. Rev. Lett.* **90**, 050401 (2003).
- [57] D. P. DiVincenzo, M. Horodecki, D. W. Leung, J. A. Smolin, and B. M. Terhal, *Phys. Rev. Lett.* **92**, 067902 (2004).
- [58] G. Adesso and A. Datta, *Phys. Rev. Lett.* **105**, 030501 (2010).
- [59] J. Maziero, H. Guzman, L. Céleri, M. Sarandy, and R. Serra, *Phys. Rev. A* **82**, 012106 (2010).
- [60] S. Hill and W. K. Wootters, *Phys. Rev. Lett.* **78**, 5022 (1997).
- [61] W. K. Wootters, *Phys. Rev. Lett.* **80**, 2245 (1998).
- [62] W. K. Wootters, *Quantum Inf. Comput.* **1**, 27 (2001).
- [63] K. A. Dennison and W. K. Wootters, *Phys. Rev. A* **65**, 010301 (2001).

Supplementary material for “Multifractality, mutual information and entanglement in the Dicke model”

Pragna Das and Auditya Sharma  
*Indian Institute of Science Education and Research Bhopal 462066 India*

arXiv:2109.06227v1 [cond-mat.stat-mech] 13 Sep 2021

## QUANTUM PHASE TRANSITION

The quantum phase transition in the Dicke model is profitably studied with the aid of a number of quantities. While the most characteristic ones are presented in the main Letter, we show some useful ancillary quantities here in the supplementary section.

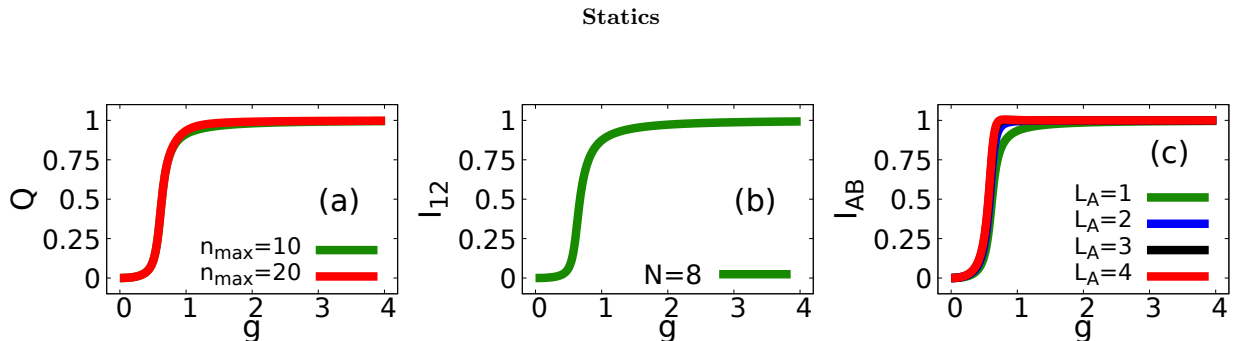


Figure 1: (a) The Meyer and Wallach  $Q$  measure of the ground state as a function of coupling,  $g$ . Number of spins  $N = 8$ . (b) Mutual information between two spins. (c) Mutual information between two spin sub-sectors. Here we divide the spins into two sub-sectors with spin number  $L_A$  and  $L_B$ . The total number of spins can be broken into  $N = 8 = L_A + L_B = 1 + 7 = 2 + 6 = 3 + 5 = 4 + 4$ . For (b) and (c)  $n_{\max} = 10$ .

The so-called Meyer and Wallach  $Q$  measure [1–4] defined as:

$$Q = 2 [1 - \text{Tr}(\rho_1^2)], \quad (1)$$

provides a useful signature at the QPT. In Fig. 1(a) we exhibit the  $Q$ -measure for the ground state of the system as a function of coupling parameter  $g$ . Here  $\rho_1$  is the single atomic reduced density matrix and it can be calculated by tracing out the bosonic part first and then over the  $N - 1$  atoms.  $Q$  is close to zero for  $g < g_c$  (NP) and close to one for  $g > g_c$  (SP) with a transition near the critical point. It goes to zero when  $\text{Tr}(\rho_1^2) \approx 1$  i.e., in the NP the single atom reduced density matrix behaves like a pure state having the two eigenvalues close to 1 and 0. On the other hand  $Q \approx 1$ , when  $\text{Tr}(\rho_1^2) \approx 0.5 < 1$ , hence  $\rho_1$  is a mixed state in the SP.

The mutual information  $I_{12}$  between two spins  $S_1$  and  $S_2$  is given by

$$\begin{aligned} I_{12} &= S_1 + S_2 - S_{12} \\ S_{1,2} &= -\text{Tr}(\rho_{1,2} \ln(\rho_{1,2})) \\ S_{12} &= -\text{Tr}(\rho_{12} \ln(\rho_{12})) \end{aligned} \quad (2)$$

where  $\rho_1, \rho_2$  are the reduced density matrices for the single spins and  $S_1, S_2$  the corresponding von Neumann entropies, while  $\rho_{12}$  is the reduced density matrix of two spins and  $S_{12}$  is the corresponding entropy. Fig. 1(b) shows the mutual information between two spins of the Dicke model.  $I_{12}$  is close to zero in the NP and close to one in the SP with a transition near the critical point. Hence we can say that the total correlation between two spins is zero in the NP whereas in the SP the correlation is maximum. Thus  $I_{12}$  significantly depends on the spin boson coupling  $g$ . Fig. 1(c) shows the mutual information between two groups of spins A and B, in which group A contains  $L_A$  spins while group B contains the remaining  $L_B = N - L_A$  spins. Because of the symmetry in the coupling it does not matter which  $L_A$  spins are considered. We see that this quantity too shows similar behaviour as  $I_{12}$ . From Fig. 1(a) we conclude that in the NP each spin is separately in a pure state, so there are no quantum correlations at all. On the other hand in the SP, we see that all the correlations are very high.

## Dynamics

We next describe how the quantum phase transition in the Dicke model is usefully studied with a quenching protocol. In a quantum quench, we prepare a closed system in an eigenstate of one Hamiltonian  $\mathcal{H}_0$  and then have the system



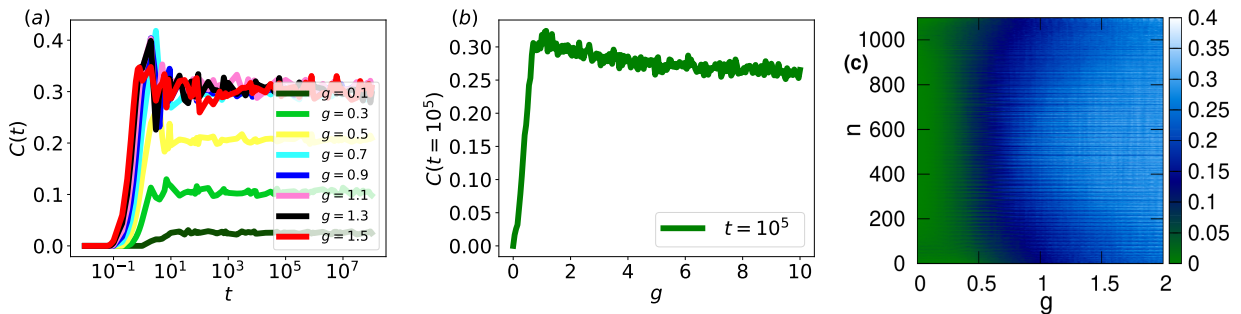


Figure 2: (a) Concurrence between two atoms as a function of time  $C(t)$  for different coupling strengths. (b) Saturation value of concurrence at time  $t = 10^5$  as a function of coupling strength  $g$ . The parameters for (a) and (b) are  $N = 128$ ,  $n_{max} = 32$ . (c) Quench dynamics of concurrence  $C$ , at time  $t = 10^6$ .  $C(t = 10^6)$  as a function of coupling parameter  $g$  and  $n$  (index for the eigenstates of the decoupled Hamiltonian  $\mathcal{H}_0$  accordingly). Green color denotes NP and blue color denotes SP. Parameters are  $N = 128$ ,  $n_{max} = 16$ .

evolve dynamically in time under a different Hamiltonian  $\mathcal{H} = \mathcal{H}_0 + \mathcal{H}_1$ . For our problem, we take  $\mathcal{H}_0$  to be the Dicke model with  $g = 0$ , and the middle excited state of  $\mathcal{H}_0$  as our initial state. The value of  $g$  is then suddenly changed to some other non-zero value of  $g$ , and the resulting dynamics of the system is studied. The concurrence (between any two atoms) as a function of time  $C(t)$  is shown for a range of values of  $g$  in Fig. 2(a). In general,  $C(t)$  starting from zero remains close to zero upto  $t \approx 0.1$ , after which it increases upto  $t \approx 10$ . With further increase of time, it tends to saturate to a constant with some fluctuations. This saturating value of  $C(t)$  depends on  $g$ , and carries information of the quantum phase transition. For  $g = 0.1$  (dark green color) the saturation value of concurrence is close to zero, but with increasing  $g$ , the saturation value increases gradually until a certain critical  $g_c$ . Beyond  $g_c$  (yellow color) we begin to see a saturating tendency of the saturation value itself with some fluctuations [see Fig. 2(a)]. This feature is made clearer by a plot of the saturation value of the concurrence at some late time, say  $t = 10^5$  as a function of the coupling parameter  $g$  as shown in Fig. 2(b). We observe that in the NP the saturation value is increasing with  $g$ , but after crossing the critical point  $g_c$ , in the SP it is almost independent of  $g$  i.e. the value is constant with some fluctuations. Thus we see that the dynamics too shows signatures of the quantum phase transition. In Fig. 2(c) we study the dynamics starting from each of the eigenstates of the decoupled Hamiltonian,  $\mathcal{H}_0 = \omega a^\dagger a + \omega_0 J_z$ , and evolving with the unitary time evolution operator  $U = e^{-i\mathcal{H}t}$  where  $\mathcal{H}$  is the system Hamiltonian. For a particular coupling strength  $g$ ,  $U$  is fixed but the initial states are changing hence  $|\psi_i(t)\rangle = U|\psi_i(0)\rangle = U|i\rangle$ , where  $\{|i\rangle\}$  are the eigenstates of  $\mathcal{H}_0$ . We plot the concurrence (between any pair of atoms) wrt the time evolved. We see that Fig. 2(c) shows that the dynamics is sensitive to the quantum phase transition no matter which eigenstate we start from.

## THERMAL PHASE TRANSITION

We now show how the analytical expression for the transition temperature may be obtained. Beginning with the scaled Hamiltonian described by Eqn.(4) in the main Letter, we write the partition function of the Dicke model as:

$$Z(N, T) = \sum_{s_1, \dots, s_N = \pm 1} \int \frac{d^2\alpha}{\pi} \langle s_1 \dots s_N | \langle \alpha | e^{-\beta \tilde{\mathcal{H}}} | \alpha \rangle | s_1 \dots s_N \rangle. \quad (3)$$

The expectation value of the Hamiltonian with respect to the bosonic modes is obtained in a straightforward manner:

$$\langle \alpha | \tilde{\mathcal{H}} | \alpha \rangle = \alpha^* \alpha + \sum_{j=1}^N \left[ \frac{\epsilon}{2} \sigma_j^z + \frac{\lambda}{\sqrt{N}} (\alpha + \alpha^*) \sigma_j^x \right]. \quad (4)$$

Defining

$$h_j = \frac{\epsilon}{2} \sigma_j^z + \frac{\lambda}{\sqrt{N}} (\alpha + \alpha^*) \sigma_j^x \quad (5)$$

the expectation value with respect to the spins becomes a product of single-spin expectation values:

$$\langle s_1 \dots s_N | \langle \alpha | e^{-\beta \tilde{H}} | \alpha \rangle | s_1 \dots s_N \rangle = e^{-\beta |\alpha|^2} \prod_{j=1}^N \langle s_j | e^{-\beta h_j} | s_j \rangle. \quad (6)$$

Using the above results, we can recast the partition function in the form of a double integral as:

$$\begin{aligned} Z(N, T) &= \int \frac{d^2 \alpha}{\pi} e^{-\beta |\alpha|^2} \left[ \text{Tr} e^{-\beta h} \right]^N \\ &= \int \frac{d^2 \alpha}{\pi} e^{-\beta |\alpha|^2} \left( 2 \cosh \left[ \frac{\beta \epsilon}{2} \left[ 1 + \frac{16 \lambda^2 \alpha^2}{\epsilon^2 N} \right]^{1/2} \right] \right)^N. \end{aligned} \quad (7)$$

Here  $\alpha$  is real, so  $|\alpha| = |\alpha^*|$ . Now

$$\int \frac{d^2 \alpha}{\pi} = \int_0^\infty r dr \int_0^{2\pi} \frac{d\theta}{\pi} = 2 \int_0^\infty r dr. \quad (8)$$

Defining  $y = \frac{r^2}{N}$  and

$$\phi(y) = -\beta y + \ln \left( 2 \cosh \left[ \frac{\beta \epsilon}{2} \left[ 1 + \frac{16 \lambda^2 y}{\epsilon^2} \right]^{1/2} \right] \right), \quad (9)$$

we have:

$$Z(N, T) = N \int_0^\infty dy \exp \left( N \phi(y) \right). \quad (10)$$

Since we are interested in the thermodynamic limit where  $N \rightarrow \infty$ , we can invoke Laplace's method [5], and the integral is given by

$$Z(N, T) = N \frac{C}{\sqrt{N}} \max_{0 \leq y \leq \infty} \exp \left( N \left[ \phi(y) \right] \right) \quad (11)$$

where  $C$  is some constant. To find the maximum of the function  $\phi(y)$ , we compute its derivative:

$$\phi' = -\beta + \frac{\beta 4 \lambda^2}{\epsilon} \frac{1}{\eta} \tanh \left( \frac{\beta \epsilon \eta}{2} \right) \quad (12)$$

where

$$\eta = \left[ 1 + \frac{16 \lambda^2 y}{\epsilon^2} \right]^{1/2}. \quad (13)$$

Putting

$$\phi' = 0, \quad (14)$$

we get

$$\eta = \frac{4 \lambda^2}{\epsilon} \tanh \left( \frac{\beta \epsilon \eta}{2} \right). \quad (15)$$

The hyperbolic tangent function is a monotonically increasing function and is bounded above by unity. Since  $\eta \geq 1$  by definition (Eqn. 13), if  $4 \lambda^2 < \epsilon$ , there is no solution for Eqn. 15. On the other hand, for  $4 \lambda^2 > \epsilon$ , the solution depends on the value of  $\beta$ . The critical value of the inverse temperature  $\beta_c$  can be computed by putting  $\eta = 1$  and is given by:

$$\beta_c = \frac{2}{\epsilon} \tanh^{-1} \left( \frac{\epsilon}{4 \lambda^2} \right). \quad (16)$$

Thus substituting  $\epsilon = \frac{\omega_0}{\omega}$  and  $\lambda = \frac{g}{\omega}$ , we have an exact expression for the transition temperature:

$$T_c = \frac{1}{\beta_c} = \left( \frac{\omega_0}{2\omega} \right) \frac{1}{\tanh^{-1} \left( \frac{\omega \omega_0}{4g^2} \right)}. \quad (17)$$

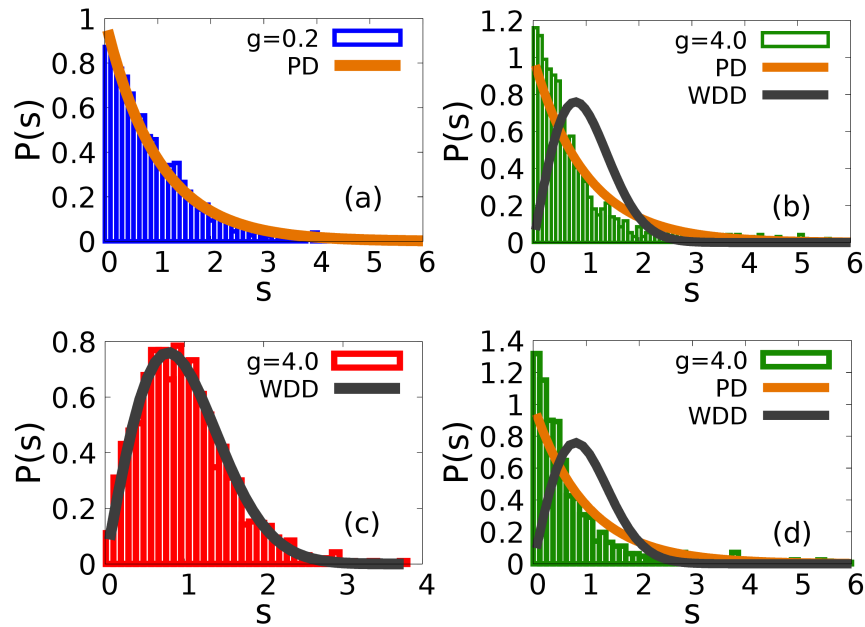


Figure 3: Level statistics of the spectrum. (a) For  $g < g_c$  the level spacing distribution is more like Poissonian. For  $g > g_c$  there are three bands in the spectrum: below the lower cut-off energy (b), above the upper cut-off energy (d), and the energies in between (c). The energy spacing distribution in between the lower and upper cut-off is more like Wigner-Dyson. However in (b), (d) the behaviours are not clear, as they show mixed behaviour, although they are closer to Poissonian behaviour.

### EXCITED STATE QUANTUM PHASE TRANSITION (ESQPT)

The Dicke model exhibits an excited state quantum phase transition in the super-radiant phase. When  $g > g_c$ , while it is well known [6, 7] that the eigenvalues above a cut-off energy  $E_c$  behave in a distinctly different manner in comparison with the eigenvalues below the cut-off, we report that in fact there is not just a lower cut-off, but also an upper cut-off. While the main Letter describes several properties connected to eigenstates, here we show *eigenvalue* data that suggest that the central band of energy levels between a lower and upper cut-off behave differently from the lower and upper energy bands.

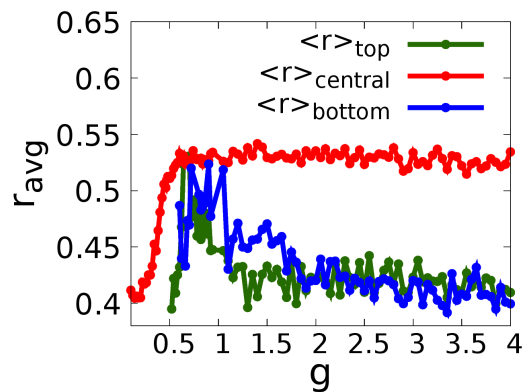


Figure 4:  $r_{avg}$  value as a function of coupling, for the different energy bands. (i) Blue color is used for energies below the lower cutoff, (ii) green color for energies above the upper cutoff, and (iii) red color for the middle band energies. Parameters are  $n_{max} = 200$ ,  $N = 60$ .

The onset of ergodic behaviour is typically diagnosed by inspection of the level spacing distribution [8]. Let  $\{E_n\}$  denote the energy levels of the DM in ascending order. Under the assumption that the density of states equals unity, the distribution  $P(s)$  of the level spacings  $s_n = E_{n+1} - E_n$  is given by the Poisson distribution  $P(s) = \exp(-s)$  in the normal phase [9]. On the other hand, in the super-radiant phase, the level spacings adhere to the Wigner-Dyson distribution  $P(s) = \frac{\pi}{2}s \exp\left[-(\pi/4)s^2\right]$  [10]. To study the level statistics we consider two  $g$  values:  $g = 0.2 < g_c$  and  $g = 4.0 > g_c$ . For  $g < g_c$  we see that the energy spacings are consistent with the Poisson distribution (PD). For  $g > g_c$  we study the level statistics separately in three bands as shown in Fig. 3. While the energy spacing distribution for levels that lie between the lower and upper cut-off energies is like the Wigner-Dyson distribution, the level spacing distributions of the upper and lower energy bands show mixed behaviour, although the distribution looks more Poissonian than Wigner-Dyson. Evidently, there is a striking absence of level repulsion in these bands, in stark contrast to the levels in the central band. While the presence of the lower cut-off is reported in the literature [6, 7], our data clearly reveal an upper cut-off as well.

The above picture with respect to the energy levels is further strengthened by a study of the ratio of consecutive level spacings, which has now become a standard measure [11]. Let  $s_n$  denote level spacing between two consecutive energies  $E_{n+1}$  and  $E_n$ . The average spacing ratio  $\langle r \rangle$  is defined as the average over  $n$  of the ratio of consecutive level spacings:

$$r_n = \frac{\min(s_{n-1}, s_n)}{\max(s_{n-1}, s_n)}. \quad (18)$$

From random matrix theory it is known that [11]  $\langle r \rangle$  takes a value  $\langle r \rangle \approx 0.386$  for quasi-integrable Hamiltonians and  $\langle r \rangle \approx 0.5307$  for Hamiltonians from the Gaussian orthogonal ensemble (GOE). For  $g < g_c$   $\langle r \rangle \approx 0.386$  and for  $g > g_c$   $\langle r \rangle \approx 0.5307$  for the central band. For the upper and the lower energy bands  $\langle r \rangle$  lies in between 0.386 and 0.5307. However, we observe that as the coupling strength increases, and as the atomic number becomes large, they tend to resemble the Poissonian ensemble [see Fig. 4].

- 
- [1] J. Karthik, Auditya Sharma, and Arul Lakshminarayan. Entanglement, avoided crossings, and quantum chaos in an ising model with a tilted magnetic field. *Phys. Rev. A*, 75:022304, Feb 2007.
  - [2] A. J. Scott. Multipartite entanglement, quantum-error-correcting codes, and entangling power of quantum evolutions. *Phys. Rev. A*, 69:052330, May 2004.
  - [3] Roya Radgohar and Afshin Montakhab. Global entanglement and quantum phase transitions in the transverse xy heisenberg chain. *Phys. Rev. B*, 97:024434, Jan 2018.
  - [4] Udaysinh T. Bhosale and M. S. Santhanam. Signatures of bifurcation on quantum correlations: Case of the quantum kicked top. *Phys. Rev. E*, 95:012216, Jan 2017.
  - [5] Harold Jeffreys, Bertha Jeffreys, and Bertha Swirls. *Methods of mathematical physics*. Cambridge university press, 1999.
  - [6] P. Pérez-Fernández, A. Relaño, J. M. Arias, P. Cejnar, J. Dukelsky, and J. E. García-Ramos. Excited-state phase transition and onset of chaos in quantum optical models. *Phys. Rev. E*, 83:046208, Apr 2011.
  - [7] R.J Lewis-Swan, Arghavan Safavi-Naini, John J Bollinger, and Ana M Rey. Unifying scrambling, thermalization and entanglement through measurement of fidelity out-of-time-order correlators in the dicke model. *Nature communications*, 10(1):1–9, 2019.
  - [8] Didier Poilblanc, Timothy Ziman, Jean Bellissard, Frederic Mila, and Gilles Montambaux. Poisson vs. goe statistics in integrable and non-integrable quantum hamiltonians. *EPL (Europhysics Letters)*, 22(7):537, 1993.
  - [9] Michael Victor Berry and Michael Tabor. Level clustering in the regular spectrum. *Proceedings of the Royal Society of London. A. Mathematical and Physical Sciences*, 356(1686):375–394, 1977.
  - [10] O. Bohigas, M. J. Giannoni, and C. Schmit. Characterization of chaotic quantum spectra and universality of level fluctuation laws. *Phys. Rev. Lett.*, 52:1–4, Jan 1984.
  - [11] Y. Y. Atas, E. Bogomolny, O. Giraud, and G. Roux. Distribution of the ratio of consecutive level spacings in random matrix ensembles. *Phys. Rev. Lett.*, 110:084101, Feb 2013.